

# Global Bottom-Up Fossil Fuel Fugitive Methane and Ethane Emissions Inventory for Atmospheric Modeling

Stefan Schwietzke,<sup>\*,†</sup> W. Michael Griffin,<sup>†,‡</sup> H. Scott Matthews,<sup>†,§</sup> and Lori M. P. Bruhwiler<sup>||</sup>

<sup>†</sup>Department of Engineering and Public Policy, Carnegie Mellon University, Baker Hall 129, 5000 Forbes Avenue, Pittsburgh, Pennsylvania 15213, United States

<sup>‡</sup>Tepper School of Business, Carnegie Mellon University, 5000 Forbes Avenue, Pittsburgh, Pennsylvania 15213, United States

<sup>§</sup>Department of Civil and Environmental Engineering, Carnegie Mellon University, Porter Hall 123A, 5000 Forbes Avenue, Pittsburgh, Pennsylvania 15213, United States

<sup>||</sup>NOAA Earth Systems Research Laboratory, 325 Broadway GMD1, Boulder, Colorado 80305, United States

## S Supporting Information

**ABSTRACT:** Natural gas (NG)-related fugitive methane ( $\text{CH}_4$ ) emissions estimates from life cycle assessments (LCA) and local field measurements are highly uncertain. Globally distributed long-term atmospheric measurements and top-down modeling can help understand whether LCA and field studies are representative of the global industry average. Attributing sources, such as the NG industry, to global total top-down emissions estimates requires detailed and transparent global *a priori* bottom-up emissions inventories. Establishing an *a priori* bottom-up inventory as a tool for top-down modeling is the focus of this work, which extends existing fossil fuel (FF) inventories over the past three decades: (i) It includes ethane ( $\text{C}_2\text{H}_6$ ) emissions, which is a convenient FF tracer gas given available global  $\text{C}_2\text{H}_6$  observations. (ii) Fuel specific  $\text{CH}_4$  and  $\text{C}_2\text{H}_6$  emissions uncertainties are quantified. (iii) NG  $\text{CH}_4$  and  $\text{C}_2\text{H}_6$  emissions are estimated for different fugitive emissions rate (FER; % of dry production) scenarios as a basis for quantifying global average FER top-down. While our global oil and coal  $\text{CH}_4$  estimates coincide well with EDGAR v4.2 for most years, country-level emissions vary substantially, and coal emissions increase at a lower rate over the past decade. Global emissions grid maps are presented for use in top-down modeling.

**KEYWORDS:** Natural gas, Methane, Life cycle assessments, Fossil fuels, Atmospheric modeling



## INTRODUCTION

Fossil fuel (FF) production, processing, transport, distribution, and final use account for about one-third of global anthropogenic emissions of methane ( $\text{CH}_4$ )<sup>1</sup>—the second largest greenhouse gas (GHG) contributor to climate change after  $\text{CO}_2$ .<sup>2</sup> Over the past three decades, global natural gas (NG) and coal production have doubled, and oil production has increased by about 50%.<sup>3</sup> Recent studies in the United States have raised concerns that NG fugitive emissions rates (FER)—the fraction of produced NG (mainly  $\text{CH}_4$ ) escaped to the atmosphere—could range between 1–9%.<sup>4–9</sup> Schwietzke et al.<sup>10</sup> used this work's bottom-up inventory as a tool in top-down atmospheric modeling to estimate globally representative FER constrained by measurements from a global observation network over the past three decades. In global top-down atmospheric modeling, global total  $\text{CH}_4$  emissions from natural and anthropogenic sources are estimated based on well-known atmospheric  $\text{CH}_4$  concentrations.<sup>11</sup> The total top-down emissions estimates are then attributed to individual emissions sources, such as the NG industry, using (i) spatial and seasonal differences in  $\text{CH}_4$  concentrations (for instance, wetland  $\text{CH}_4$  emissions follow a seasonal cycle) and (ii) Bayesian *a priori*

estimates of the approximate emissions quantities and locations of each source.<sup>12</sup> *A priori* estimates (first best estimates based on process models; henceforth *priors*) are summarized in bottom-up inventories, such as the Emissions Database for Global Atmospheric Research (EDGAR)<sup>13</sup> and the Greenhouse Gas and Air Pollution Interactions and Synergies (GAINS) Model.<sup>14</sup> Studies<sup>12,15,16</sup> have shown that source attribution relies heavily on *priors* in regions where several different  $\text{CH}_4$  sources are in close proximity to each other. The accuracy of the emissions source attribution therefore depends strongly on the quality of the *prior* bottom-up inventory, which calls for a high degree of transparency in inventory data and methods.<sup>10,12</sup> When *prior* uncertainties are not reported (e.g., in EDGAR,<sup>13</sup> one of the most widely used databases for top-down modeling), top-down modelers need to set *prior* uncertainties somewhat arbitrarily. The aim of this paper is to provide a transparent description of a *prior* bottom-up inventory including uncertainties developed for top-down modeling, which can be

Received: March 6, 2014

Revised: May 3, 2014

Published: June 19, 2014

improved as more information becomes available. Establishing global FF CH<sub>4</sub> emissions inventories is also important for better understanding the global CH<sub>4</sub> cycle<sup>12,17</sup> and for estimating mitigation potentials and costs.<sup>14,18</sup>

Previous studies have generated global bottom-up FF CH<sub>4</sub> emissions inventories.<sup>13,14,18</sup> In addition to FF, these studies have estimated global CH<sub>4</sub> emissions from other anthropogenic sources, such as agriculture and waste. The EDGAR and GAINS databases by Janssen-Maenhout et al.<sup>19</sup> and Höglund-Isaksson,<sup>14</sup> respectively, also decomposed global emissions estimates into grid maps, that is, assigning spatial emissions distributions for atmospheric modeling. The global CH<sub>4</sub> emissions inventory and grid maps described here extend previous work<sup>13,14</sup> in three important ways. First, this paper estimates ethane (C<sub>2</sub>H<sub>6</sub>) emissions—the second most abundant FF hydrocarbon component—in addition to CH<sub>4</sub>. Given the literature data for coal, oil, and NG specific CH<sub>4</sub>/C<sub>2</sub>H<sub>6</sub> composition ratios summarized in this work, the FF C<sub>2</sub>H<sub>6</sub> inventory is useful in top-down atmospheric modeling for estimating FER using global C<sub>2</sub>H<sub>6</sub> observations as an additional observational constraint. Using the present inventory, Schwietzke et al.<sup>10</sup> have shown that the upper-bound global average FER can be determined with greater confidence using global average C<sub>2</sub>H<sub>6</sub> concentrations compared with CH<sub>4</sub>. Second, this study presents FF emissions uncertainties, which received little attention in previous global *prior* bottom-up inventories used in global top-down CH<sub>4</sub> modeling. For example, emissions uncertainties are not available in the EDGAR database,<sup>13</sup> which was used in most previous global top-down atmospheric modeling studies.<sup>12,15,16,20–23</sup> Information about uncertainties is particularly important for distinguishing NG from oil and coal. If, for instance, *prior* oil and coal emissions were underestimated, this error would bias the emissions source allocation in the top-down modeling, that is, NG emissions were overestimated.<sup>10</sup> Finally, this work estimates total NG CH<sub>4</sub> and C<sub>2</sub>H<sub>6</sub> emissions for different FER scenarios, for example, absolute CH<sub>4</sub> emissions per % of produced NG emitted to the atmosphere. This is important because top-down atmospheric modeling *per se* can only estimate absolute emissions, and this work facilitates converting the top-down estimates to FER,<sup>10</sup> which allows comparison with recent FER estimates in the United States.<sup>4–9</sup> Top-down modeling using *prior* estimates from EDGAR prohibits such comparison due to insufficient transparency of data and methods, which was a major motivation for developing this inventory.

## METHODS

Estimation of global FF CH<sub>4</sub> and C<sub>2</sub>H<sub>6</sub> emissions follows the general structure in Figure 1. More details about the literature data described in this section are provided in the Supporting Information. Global NG emissions were estimated based on FER scenarios (ranging from 1 to 9%; section 3, Supporting Information), dry production data (referring to consumer grade NG; Table S-2, Supporting Information), and downstream NG CH<sub>4</sub> and C<sub>2</sub>H<sub>6</sub> content (post-processing; Table S-2, Supporting Information). Using dry production in combination with the downstream NG CH<sub>4</sub> and C<sub>2</sub>H<sub>6</sub> content is appropriate by U.S. Energy Information Administration (EIA) definitions,<sup>24</sup> and it allows comparing FER results with many previous studies (see literature review in section 3, Supporting Information), which also used dry production as a basis. The downstream NG composition was estimated in a mass balance due to lack of publicly available data. Global oil CH<sub>4</sub> emissions and uncertainties were estimated using literature emissions factors (EF), which include (i) unintentional

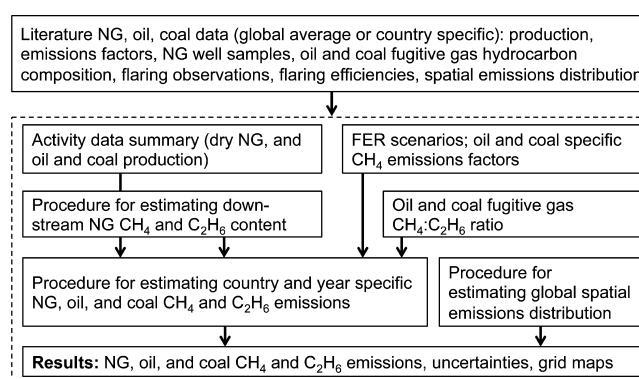


Figure 1. Methods section overview and structure.

fugitive emissions throughout the life cycle, (ii) CH<sub>4</sub> emitted from venting of associated gas<sup>25</sup> at oil wells, and (iii) incomplete flaring (for converting CH<sub>4</sub> to CO<sub>2</sub>). Note that EFs could include potential geological emissions,<sup>26</sup> and the implications for global NG and oil emissions are discussed in more detail in Schwietzke et al.<sup>10</sup> Global coal CH<sub>4</sub> emissions and uncertainties were estimated using literature (i) EFs from underground and surface mining as well as post-mining activities and abandoned mine emissions, and (ii) coal production data from underground and surface mining for major coal producing countries. Literature data on CH<sub>4</sub>:C<sub>2</sub>H<sub>6</sub> ratios (gas composition) in fugitive gases from oil and coal production were used to estimate global oil and coal C<sub>2</sub>H<sub>6</sub> emissions because EFs for C<sub>2</sub>H<sub>6</sub> are typically not available. On the basis of these estimates, grid maps were developed for atmospheric modeling, which can be used to improve the emissions estimates with global atmospheric measurements over time.<sup>10,12,27</sup>

## ACTIVITY DATA

The amount of fuel produced in a given year and/or country (activity data) is used for generating the emissions time series of a given fuel in combination with the associated EFs. EIA<sup>3</sup> international NG, oil, and coal production data was used here, and differences between EIA and other sources are discussed in section 1 of the Supporting Information. China is the world's largest coal producer, accounting for 53% of global underground coal production from 1980–2010.<sup>3</sup> Illegal coal production may be about 10% of the reported total production,<sup>28</sup> that is, total reported Chinese coal production<sup>3</sup> could be underestimated. Two other sources<sup>29,30</sup> indicate a significant coal production data mismatch among different Chinese government agencies, also suggesting that the EIA coal production data during 1997–2008 are underestimated. Aden<sup>29</sup> was used for this period as a conservative estimate, while Guan et al.<sup>30</sup> report that Chinese coal production may in fact be higher.

Country specific FF *production* data are only a proxy for the spatial distribution of emissions. Emissions may not always be released in the country where fuel *extraction* occurred. The vast majority of coal- (Table 2) and oil-related CH<sub>4</sub> emissions occur at the extraction site, thus using *production* statistics is reasonable. A fraction of CH<sub>4</sub> emissions from NG produced in Russia, for instance, may be released in Central European local distribution systems where it is transported via pipelines. Many recent LCA studies<sup>4,6,31</sup> estimate combined transportation and distribution losses of less than 1% FER but others<sup>32,33</sup> report significantly higher values before the mid-1990s (see Table S-9, Supporting Information, for a literature review of downstream FER estimates). A share of the pipeline emissions and all of the distribution-related emissions of this

NG are therefore associated with the NG consumption data of the importing country as well as any country where the pipeline transits (section 1, Supporting Information). It is assumed here that all emissions occur in the country where the FFs are produced due to lack of data and given the uncertainties associated with the spatial allocation of CH<sub>4</sub> emissions in the grid maps as described in more detail in the Results section.

### ■ ESTIMATING DOWNSTREAM NATURAL GAS HYDROCARBON COMPOSITION

Apart from a few samples collected in the 1960s,<sup>34</sup> there are no recent publicly available data providing nationally or internationally representative downstream NG composition. Literature upstream (prior to NG processing; see Table S-2, Supporting Information) and downstream NG composition data around the world are summarized in Table S-4 of the Supporting Information. This global NG composition survey and the assessment of uncertainties below improve previous work, which either do not document composition<sup>13</sup> or use a discrete value.<sup>14</sup> Downstream NG composition was estimated by performing a mass balance of United States NG upstream and downstream of processing, that is, upstream NG volume equals downstream NG volume plus natural gas liquids (NGL) separated during NG processing. For upstream NG volumes, we used EIA<sup>35</sup> marketed production statistics (well gas minus repressured and flared/vented gas, and nonhydrocarbon gases, mainly nitrogen (N<sub>2</sub>) and carbon dioxide (CO<sub>2</sub>) removed).<sup>24</sup> For downstream NG volumes, we used EIA<sup>35</sup> dry production statistics, that is, marketed production minus NGLs removed during NG processing.<sup>24</sup>

Mass balance eqs 1–8 are given below, where  $V_{up,x,i}$  and  $V_{up,CH_4,i}$  are absolute upstream NG volume streams (at 1.015 bar and 289 K<sup>24</sup>) of component  $x$  (C<sub>2</sub>H<sub>6</sub>, propane, butane) and CH<sub>4</sub>, respectively, in year  $i$ ;  $VF_{up,x}$  and  $VF_{up,CH_4}$  are upstream NG volume fractions from two NG composition databases<sup>36,37</sup> described below;  $P_{mark,i}$  and  $P_{dry,i}$  are marketed and dry production (in m<sup>3</sup>), respectively;  $V_{down,x,i}$  and  $V_{down,CH_4,i}$  are the absolute downstream NG volume streams;  $NGL_{x,i}$  is the absolute NG liquids volume stream of component  $x$ ;<sup>38</sup>  $VF_{down,x,i}$  and  $VF_{down,CH_4,i}$  are downstream NG volume fractions; and  $WF_{down,x,i}$  and  $WF_{down,CH_4,i}$  are downstream NG weight fractions using the gas densities  $\rho_x$  in Table S-3 of the Supporting Information. Since pentane and hexane (i) contribute less than 1 mol % to NG<sup>36,37</sup> and (ii) are often not reported (thus reducing sample size),<sup>36,37</sup> they were omitted from the mass balance.

$$V_{up,x,i} = VF_{up,x} \times P_{mark,i} \quad (1)$$

$$V_{up,CH_4,i} = VF_{up,CH_4} \times P_{mark,i} \quad (2)$$

$$V_{down,x,i} = (V_{up,x,i} - NGL_{x,i}) \quad (3)$$

$$V_{down,CH_4,i} = P_{dry,i} - \sum_x V_{down,x,i} \quad (4)$$

$$VF_{down,x,i} = \frac{V_{down,x,i}}{V_{down,i}} \quad (5)$$

$$VF_{down,CH_4,i} = \frac{V_{down,CH_4,i}}{V_{down,i}} \quad (6)$$

$$WF_{down,x,i} = \frac{VF_{down,x,i} \times \rho_x}{VF_{down,CH_4,i} \times \rho_{CH_4} + \sum_x VF_{down,x,i} \times \rho_x} \quad (7)$$

$$WF_{down,CH_4,i} = \frac{VF_{down,CH_4,i} \times \rho_{CH_4}}{VF_{down,CH_4,i} \times \rho_{CH_4} + \sum_x VF_{down,x,i} \times \rho_x} \quad (8)$$

Upstream NG hydrocarbon compositions  $VF_{up,x}$  and  $VF_{up,CH_4}$  were estimated (including uncertainties) using two databases. The U.S. Bureau of Land Management (BLM) database<sup>37</sup> contains routine analyses of United States and international oil and gas well hydrocarbon composition (among others) collected as part of a continuous survey for occurrences of helium. This survey was conducted from 1917 until 1997 and consists of 17,167 samples analyzed for hydrocarbons and other components (mainly N<sub>2</sub> and CO<sub>2</sub>). The second database was provided by Etiope<sup>36</sup> and contains 1363 NG samples collected globally, mostly between 1984 and 1997. Because the mass balance requires composition data for all NG components in eqs 1–8, those samples missing one or more entries were removed. As described in more detail in section 2 of the Supporting Information, other data challenges included identifying samples from nonproducing wells and other inconsistencies (e.g., sample date after publication date). After screening both databases for erroneous/missing entries, a total of 6989 NG samples (Table S-5, Supporting Information) were used for estimating  $VF_{up,x}$  and  $VF_{up,CH_4}$ . It is assumed that the literature well gas samples<sup>36,37</sup> are representative of upstream NG directly prior to processing. While there is significant spatial variability in upstream NG composition within each basin, framing uncertainty in terms of confidence intervals from all samples was deemed sufficient for this global- and national-level analysis. Nonhydrocarbons (especially N<sub>2</sub> and CO<sub>2</sub>) reported in the sample data were excluded from the mass balance to represent the fact that nonhydrocarbons are already removed in marketed production data.<sup>24</sup>

### ■ COUNTRY-SPECIFIC NATURAL GAS, OIL, AND COAL CH<sub>4</sub> AND C<sub>2</sub>H<sub>6</sub> EMISSIONS

**Natural Gas.** Natural gas and oil CH<sub>4</sub> and C<sub>2</sub>H<sub>6</sub> emissions were estimated for 37 and 26 countries with best available data (representing 96% and 91% of 1980–2011 world production), respectively (Table S-1, Supporting Information). Emissions estimates for the remaining countries were adopted from EDGAR v4.2.<sup>13</sup> Estimates were generated for the past three decades to be used as *priors* in atmospheric modeling<sup>10</sup>—the period for which global observational data<sup>12,27</sup> is available.

Country-specific absolute NG industry CH<sub>4</sub> and C<sub>2</sub>H<sub>6</sub> emissions  $E_{NG,CH_4,i}$  and  $E_{NG,C_2H_6,i}$  in year  $i$  were estimated using eq 9 and eq 10 based on fugitive emissions rate  $FER_{NG,i}$  (percentage of dry production emitted) and dry production  $P_{dry,i}$  (converted to Tg/year using the chemical properties in Table S-3, Supporting Information). Note that the FER scenarios in this work include total NG industry emissions, whereas the GAINS model<sup>14</sup> uses EFs for different life cycle stages (EFs are not documented in EDGAR<sup>13</sup>). Emissions for FER scenarios were estimated for use in top-down modeling (based on observational constraints) in order to confine the reported<sup>4–9</sup> wide uncertainty range of total FER (1–9%). NG industry emissions were estimated for several scenarios including (i) constant FER across world regions and time and (ii) regionally distinct FER with a decline over time (Table

Table 1. Summary of Oil CH<sub>4</sub> Emissions Factors from Four Different Studies

	EF (kg CH <sub>4</sub> /m <sup>3</sup> oil)	notes; see section 4, Supporting Information, for details	ref
EPA 2013			
average (1990–2010)	2.9	based on reported total emissions and EIA <sup>44</sup> oil production statistics	40
95% C.I., low	2.2		
95% C.I., high	7.2		
Wilson et al. 2004, 2008			
low	0.8	same as EPA; required oil/NG allocation	41, 42
high	6.9		
IPCC 2006			
developed world (weighted average)	11	–	43
developing world low	11		
developing world high	41		

S-17, Supporting Information). The FER decline is consistent with recent top-down studies,<sup>27,39</sup> which also find decreasing FF emissions over time. Scenarios range from 1–9% FER given our literature review from 16 studies (Table S-9, Supporting Information), which have either (i) directly incorporated EFs from industry or government sources or life cycle assessment (LCA) databases or (ii) reported original measurements. FER refers to the percentage of produced NG emitted to the atmosphere throughout NG production, processing, pipeline transport, and local distribution.

A weighted average downstream and upstream NG C<sub>2</sub>H<sub>6</sub> weight fraction would be needed to reflect that (i) a significant portion of C<sub>2</sub>H<sub>6</sub> is removed in the downstream gas and (ii) the ratio between upstream and downstream FER is not necessarily 1:1 and is highly uncertain (Table S-4, Supporting Information). Due to data unavailability, downstream NG C<sub>2</sub>H<sub>6</sub> weight fraction was used in this study. This choice underestimates the total NG C<sub>2</sub>H<sub>6</sub> emissions at a given NG loss to the atmosphere because upstream NG C<sub>2</sub>H<sub>6</sub> content is higher compared to downstream NG. As a result, this choice overestimates FER in atmospheric modeling<sup>10</sup> (FER = top-down NG C<sub>2</sub>H<sub>6</sub> emissions estimate ÷ (dry production × downstream NG C<sub>2</sub>H<sub>6</sub> content)), which is convenient for estimating an upper-bound FER.

$$E_{NG,CH_4,i} = FER_{NG,i} \times P_{dry,i} \times WF_{down,CH_4,i} \quad (9)$$

$$E_{NG,C_2H_6,i} = FER_{NG,i} \times P_{dry,i} \times WF_{down,C_2H_6,i} \quad (10)$$

**Oil.** Country-specific absolute oil industry CH<sub>4</sub> emissions  $E_{Oil,CH_4,i}$  in year  $i$  (eq 11) were estimated based on emissions factor  $EF_{Oil,CH_4}$ , oil production  $P_{Oil,i}$  (in m<sup>3</sup> oil/year), flaring efficiency  $EF_{Flare}$ , associated (flared) gas CH<sub>4</sub> content  $WF_{assoc,flare,CH_4}$  and observed flaring amount  $P_{Flare,i}$  (in Tg NG/year; section 4, Supporting Information). Oil-related emissions in GAINS<sup>14</sup> were estimated separately for associated gas from “conventional” and “heavy” oil production, while a similar distinction was made in this inventory by accounting for uncertainty in associated gas hydrocarbon composition (related information is not documented in EDGAR<sup>13</sup>). Oil industry C<sub>2</sub>H<sub>6</sub> emissions  $E_{Oil,C_2H_6,i}$  (eq 12) were scaled from  $E_{Oil,CH_4,i}$  using the associated gas composition CH<sub>4</sub>:C<sub>2</sub>H<sub>6</sub> (wt %) ratio  $R_{oil,CH_4/C_2H_6}$  from the literature. Given the uncertainty among sources (1.7–3.3; Table S-4, Supporting Information), three ratio scenarios were chosen: low (3.3), medium (2.5), and high (1.7) C<sub>2</sub>H<sub>6</sub> content.

$$E_{Oil,CH_4,i} = EF_{oil,CH_4} \times P_{oil,i} + EF_{Flare} \times WF_{assoc,flare,CH_4} \times P_{Flare,i} \quad (11)$$

$$E_{oil,C_2H_6,i} = \frac{E_{oil,CH_4,i}}{R_{oil,CH_4/C_2H_6}} \quad (12)$$

On the basis of the literature EFs in Table 1, the U.S. Environmental Protection Agency (EPA)<sup>40</sup> was selected for the  $EF_{Oil,CH_4}$  parameter, and the other EFs<sup>41–43</sup> were used to quantify emissions uncertainties. The EPA<sup>40</sup> EF is 51% lower than the mean of the lowest<sup>41,42</sup> and highest<sup>43</sup> EF. The EPA<sup>40</sup> EF thus provides a lower bound for oil industry emissions, which is convenient for estimating an upper-bound FER (top-down NG emissions = top-down total emissions – bottom-up emissions all other sources).<sup>10</sup>

As discussed in section 4 of the Supporting Information, flaring efficiencies incorporated in the oil EFs in Table 1 appear significantly overestimated.<sup>45,46</sup> This study uses 95% flaring efficiency  $EF_{Flare}$  (versus 98% in EPA<sup>40,47</sup> and GAINS<sup>14</sup>) and 40 wt % associated (flared) NG CH<sub>4</sub> content  $WF_{assoc,flare,CH_4}$  as conservative values, that is, leading to a lower-bound of flaring emissions and NOAA<sup>48,49</sup> flaring observations  $P_{Flare,i}$ . Because observations are available only from 1994 to 2010, flaring data were extrapolated prior to 1994 based on the ratio of flaring to oil production. The ratio is relatively constant over time for most countries, and some have higher ratios in earlier years (Figure S-3, Supporting Information). The 1994 ratio was used for pre-1994, which is a conservative estimate, because the trend indicates that the ratio could be higher.

**Coal.** Coal CH<sub>4</sub> emissions were estimated for 22 countries for which separate underground and surface mining production data is available, representing 95% of the world’s primary coal production from 1980–2010 (Table S-15, Supporting Information). Country-specific absolute coal industry CH<sub>4</sub> emissions  $E_{Coal,CH_4,i}$  in year  $i$  (eqs 13–15) were estimated based on underground mining emissions factor  $EF_{Coal,i,u}$ , underground coal production  $P_{Coal,i,u}$ , surface mining emissions factor  $EF_{Coal,i,s}$ , and surface coal production  $P_{Coal,i,s}$ . Note that GAINS<sup>14</sup> also distinguishes between underground and surface coal production, but the fractions of underground/surface mining are assumed constant over time (related information is not documented in EDGAR<sup>13</sup>).  $EF_{Coal,i,u}$  is the sum of mining emissions factor  $EF_{Coal,i,u,m}$  and post-mining and abandoned mines emissions factor  $EF_{Coal,i,u,pm\&am}$ .  $EF_{Coal,i,s}$  is the sum of mining emissions factor  $EF_{Coal,i,s,m}$  and post-mining emissions factor  $EF_{Coal,i,s,pm}$ . Coal industry C<sub>2</sub>H<sub>6</sub> emissions  $E_{Coal,C_2H_6,i}$  (eq 16) were scaled from  $E_{Coal,CH_4,i}$  using the coal-bed gas composition CH<sub>4</sub>:C<sub>2</sub>H<sub>6</sub> (wt %) ratio  $R_{Coal,CH_4/C_2H_6}$  from the literature.

$$E_{Coal,i} = EF_{Coal,i,u} \times P_{Coal,i} + EF_{Coal,i,s} \times P_{Coal,i,s} \quad (13)$$

$$EF_{Coal,i,u} = EF_{Coal,i,u,m} + EF_{Coal,pm\&m} \quad (14)$$

$$EF_{Coal,i,s} = EF_{Coal,i,s,m} + EF_{Coal,pm} \quad (15)$$

$$E_{Coal,C2H6,i} = \frac{E_{Coal,CH4,i}}{R_{Coal,CH4/C2H6}} \quad (16)$$

Section 5 of the Supporting Information describes the CH<sub>4</sub>:C<sub>2</sub>H<sub>6</sub> ratio uncertainty among data sources,<sup>50,51</sup> and three ratio scenarios were chosen: low (1000), medium (100), and high (50) C<sub>2</sub>H<sub>6</sub> content. Country-specific emissions factors  $EF_{Coal,i,u}$  and  $EF_{Coal,i,s}$  are listed in Table 2 for quantifying medium estimates (third column) and lower/upper bounds (second column).

**Table 2. Summary of Literature Coal CH<sub>4</sub> Emissions Factors from Underground and Surface Mining as Well as Different Life Cycle Stages<sup>a</sup>**

	range	medium estimate	notes	refs
<i>Underground EFs</i>				
China	11–12	11 <sup>b</sup>	province-level averages	52, 53
United States	11–15	12	range [ref 43]; best estimate [ref 40]	
other major producers	6.8–24 <sup>b</sup>	n/a <sup>c</sup>	FSU <sup>d</sup> , Germany, Poland, United Kingdom, Czech Republic, Australia	43
IPCC Tier 1	10–25	18 <sup>b</sup>	globally representative values	
<i>Surface EFs</i>				
IPCC Tier 1	0.3–2.0	1.2 <sup>b</sup>	globally representative values	43
<i>Post-Mining EFs</i>				
underground	0.9–4.0	1.5	range [ref 43]; best estimate [ref 40]; Table S-13, Supporting Information	
surface	0.0–0.2	0.2		
<i>Abandoned Mine EFs</i>				
underground	1.1–1.5	1.3 <sup>b</sup>	United States data (Table S-14, Supporting Information)	40

<sup>a</sup>Units are m<sup>3</sup> CH<sub>4</sub>/t (metric ton) coal. <sup>b</sup>Mean of range. <sup>c</sup>See Table S-12 of the Supporting Information for country-specific values. <sup>d</sup>Former Soviet Union.

## ■ SPATIAL DISTRIBUTION OF COUNTRY-LEVEL EMISSIONS USING EDGAR CH<sub>4</sub> EMISSIONS GRID MAPS

The spatial distribution of country-level emissions in EDGAR's global emissions grid maps<sup>13</sup> was adopted. The distribution is based on population density, FF production sites, and

transportation routes among other proxies. Grid maps only provide approximate spatial information on emissions sources on a country or regional level. However, the spatial resolution of 3D top-down models is usually significantly lower than the grid maps due to computational efficiency constraints.<sup>12</sup> The EDGAR<sup>13</sup> grid maps were scaled for each country individually, such that the total emissions of each country in the grid map matches the country's emissions estimated above. In order to scale the countries in the NG, oil, and coal maps individually in each year, the grid cells in the EDGAR<sup>13</sup> maps belonging to each country were identified. A national identifier map was generated using raw data provided by EDGAR<sup>13</sup> (land-based national boundaries) and the Flanders Marine Institute maritime boundaries geodatabase to perform this step.<sup>54</sup> Boundaries for maritime sovereign regions were used to allocate offshore emissions to individual countries, for example, United States NG and oil drilling in the Gulf of Mexico. Emissions for the countries not estimated above (accounting for 4%, 9%, and 5% of global NG, oil, and coal production, respectively) were left unchanged from the original EDGAR data set. Individual NG, oil, and coal grid maps were generated for each year for use atmospheric modeling.<sup>10</sup> A detailed description of the grid map scaling process is provided in section 6 of the Supporting Information.

## ■ RESULTS

The results of the NG processing mass balance for estimating downstream NG composition are summarized in Table 3. It shows long-term averages (and uncertainties due to upstream gas composition) throughout 1984–2011, during which marketed, dry, and NGL production data<sup>38</sup> as well as atmospheric measurement data<sup>11</sup> is available. Over this period, NGL C<sub>2</sub>H<sub>6</sub> and marketed production increased by 83% and 32%, respectively.<sup>35,38</sup> Given this increased C<sub>2</sub>H<sub>6</sub> removal during NG processing, downstream C<sub>2</sub>H<sub>6</sub> content decreased from 7.8% in 1984 to 6.8% in 2011 (Table S-8, Supporting Information).

To ensure confidence in the results, we tested whether the CH<sub>4</sub> volume flow upstream is conserved downstream. The upstream CH<sub>4</sub> volume flow is 0.1% lower than downstream, which is a small error considering the uncertainty in the upstream NG composition (±1 vol %, 95% C.I.). Details and a summary of the upstream NG sample data from two large databases ( $N = 6989$ ) are provided in Table S-6 of the Supporting Information. Energy content of downstream NG is consistent with pipeline quality standards (far right column). Demonstrating the global representativeness of our mass balance results requires detailed international C<sub>2</sub>H<sub>6</sub>, C<sub>3</sub>H<sub>8</sub>, and C<sub>4</sub>H<sub>10</sub> production statistics, which were not available to the authors. However, as described in section 2 of the Supporting Information, we use total United States and international NGL

**Table 3. Summary of Downstream NG Composition Using a NG Upstream–Downstream Mass Balance Approach<sup>a</sup>**

	units	CH <sub>4</sub>	C <sub>2</sub> H <sub>6</sub>	C <sub>3</sub> H <sub>8</sub>	C <sub>4</sub> H <sub>10</sub>	ΔCH <sub>4</sub> (upstream–downstream) <sup>b</sup>	energy content (Btu/cft)	
							mass balance	literature <sup>c</sup>
mean	vol %	93	4.3	1.6	0.7	−0.1	1086	950–1150
mean	wt %	86	7.4	4.2	2.5			
95% C.I.	wt %	85–87	7.2–7.7	4.0–4.4	2.3–2.7	n/a	n/a	n/a

<sup>a</sup>Values are averages over the period from 1984–2011 (see Table S-8, Supporting Information, for individual years). <sup>b</sup>Difference between upstream and downstream CH<sub>4</sub> mass flow, in % of dry production (see explanation in text). <sup>c</sup>Pipeline quality standards (see section 2, Supporting Information, for details).

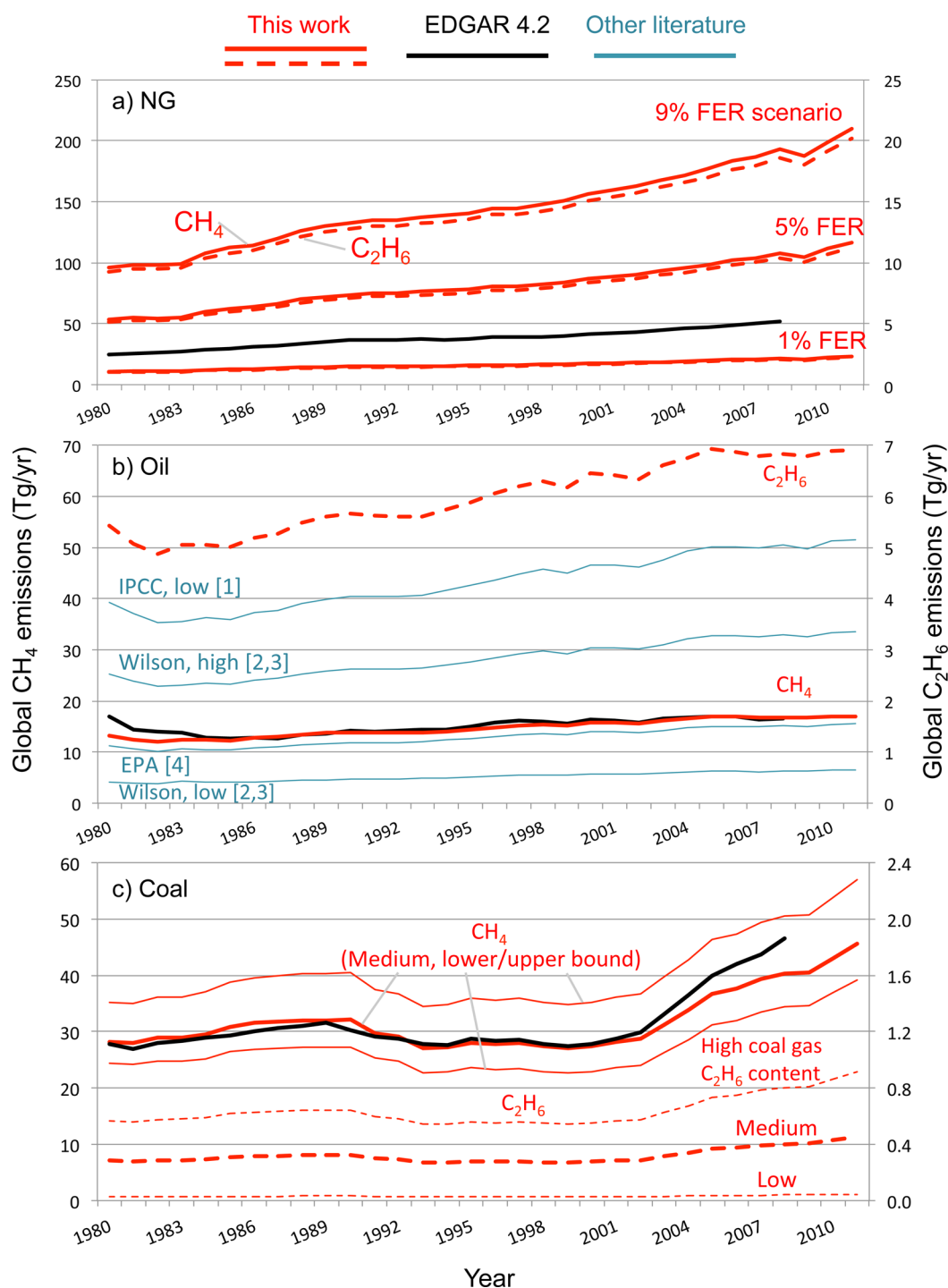


**Figure 2.** Global FF  $\text{CH}_4$  and  $\text{C}_2\text{H}_6$  emissions (red) in comparison with EDGAR (v4.2,<sup>13</sup>  $\text{CH}_4$  only, black)—the predominantly used *prior* database in global top-down studies—and other literature. Panels a, b, and c show NG, oil, and coal emissions, respectively. Solid (left axis) and dashed (right axis) lines are  $\text{CH}_4$  and  $\text{C}_2\text{H}_6$  emissions, respectively. NG  $\text{CH}_4$  emissions uncertainties are  $\pm 1\%$  of mean values (Table 3). NG and oil  $\text{C}_2\text{H}_6$  emissions are shown for mean dry and associated gas  $\text{C}_2\text{H}_6$  content, respectively (see Table S-16, Supporting Information, for uncertainties). Oil  $\text{CH}_4$  uncertainties (blue) are represented by EFs from four studies ([1] is ref 43; [2] is ref 41; [3] is ref 42; [4] is ref 40). Coal  $\text{C}_2\text{H}_6$  emissions uncertainties (low, medium, high scenarios) are as described in the Methods section.

production statistics to show that if United States and international downstream NG  $\text{C}_2\text{H}_6$  content is statistically different the global average downstream NG  $\text{C}_2\text{H}_6$  content is likely higher than in the United States. In this case, global total NG  $\text{C}_2\text{H}_6$  emissions in this inventory would be underestimated for a given FER. Analogously, FER would be overestimated in top-down modeling for a given global total  $\text{C}_2\text{H}_6$  budget, which

is convenient for quantifying an upper-bound FER (see Methods section). Thus,  $\text{C}_2\text{H}_6$ -based FER top-down results using this inventory should be regarded as high estimates until more global downstream composition data is available.

Figure 2 summarizes global  $\text{CH}_4$  and  $\text{C}_2\text{H}_6$  emissions from NG, oil, and coal over time and compares it with EDGAR v4.2<sup>13</sup> and other literature.<sup>40–43</sup> The long-term increase in

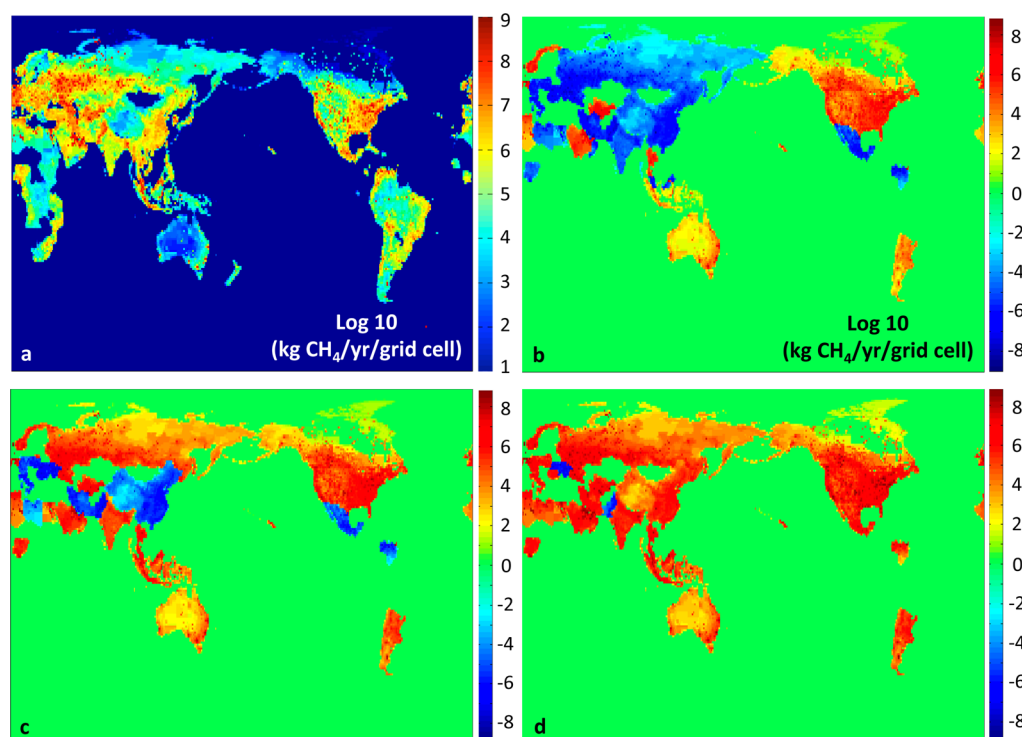


**Figure 3.** NG CH<sub>4</sub> emissions grid maps for the year 2008 in 1° × 1° resolution for use in CarbonTracker-CH<sub>4</sub>. Note that the legend units are in kg CH<sub>4</sub>/yr/grid cell on a logarithmic scale (numbers indicating exponents to base 10). Panel a shows emissions for the medium FER scenario (global average 3.1% FER; Table S-17, Supporting Information). Panels b–d illustrate emissions differences between the low (b, 2.2% global average FER), medium (c), and high (d, 5.1% global average FER) scenarios and EDGAR v4.2.<sup>13</sup> Red and blue colors indicate greater and fewer emissions than EDGAR, respectively.

emissions for all FF is due to surging production. Note that the uncertainties in Figure 2 describe the best knowledge of available data as documented in the Methods section. Uncertainties for some parameters were quantified in terms of confidence intervals due to large sample size (e.g., upstream NG composition; Table S-7, Supporting Information), whereas ranges were available for other parameters (e.g., underground coal EFs). Production data is deterministic. Thus, lack of data precludes quantifying statistically robust total emissions distributions, and this inventory can be updated as more data becomes available. NG emissions (panel a) represent different FER scenarios, which can be used in top-down modeling (based on observational constraints) in order to confine the reported<sup>4–9</sup> wide uncertainty range of total FER (1–9%). It shows constant FER across space and time (see Table S-18, SI, for details about country-level estimates). Our inventory can allow converting absolute top-down NG emissions estimates (in Tg/yr) to global average FER for comparison with recent LCA and local top-down estimates, that is, up to 9% FER.<sup>9</sup> Note that in the 9% FER scenario, NG alone accounts for 30–40% of the global CH<sub>4</sub> emissions budget compared to about 10% in the literature.<sup>1</sup> Over the past decade, C<sub>2</sub>H<sub>6</sub> emissions alone in the 9% FER scenario are greater than any global C<sub>2</sub>H<sub>6</sub> budget in the literature.<sup>27,39</sup> Top-down modeling by Schwietzke et al.<sup>10</sup> used this *prior* emissions inventory to estimate bounds on FER. The EDGAR v4.2 CH<sub>4</sub> inventory<sup>13</sup> is equivalent to about 2.5% FER. This value is not reported in EDGAR but inferred by comparing absolute emissions with this work (Figure 2). Note that country-level emissions (Table S-18, SI) vary significantly between this work and EDGAR<sup>13</sup>.

Global oil CH<sub>4</sub> and C<sub>2</sub>H<sub>6</sub> emissions are shown in panel b in comparison with emissions using other literature EFs described in Table 1. While the oil CH<sub>4</sub> results coincide closely with EDGAR<sup>13</sup> estimates, the uncertainties quantified here (shown by the blue lines, which represent EFs from four studies<sup>40–43</sup>) represent a further development. While it is difficult to ascribe an emissions distribution using four data points, this work's oil CH<sub>4</sub> estimate may be considered a conservative (lower-bound) estimate. To support this statement, note that Wilson et al.<sup>41,42</sup> reported that EF is likely an underestimate due to incomplete reporting of total emissions (section 4, Supporting Information). Also, the IPCC's<sup>43</sup> high estimate EF for developing countries (Table 1; not shown in Figure 2) is an order of magnitude higher than the EPA's<sup>40</sup> used here. Furthermore, our assumption of 95% flaring efficiency increases oil CH<sub>4</sub> emissions on average 2 Tg/yr compared to EPA<sup>40</sup> estimates (Figure 2). The increase is significant relative to the total oil CH<sub>4</sub> estimate (on average 15 Tg/yr) found here but is minor relative to total uncertainties (on average 5–43 Tg/yr). As shown in Table S-18 of the Supporting Information, country-level oil CH<sub>4</sub> emissions vary significantly between this work and EDGAR. For instance, our oil CH<sub>4</sub> emissions are over 70% and 250% higher than EDGAR (averaged over 1980–2011) for the United States and the United Kingdom, respectively. CH<sub>4</sub> emissions in other countries, such as Canada and Nigeria, are up to 60% lower than in EDGAR. Uncertainties in C<sub>2</sub>H<sub>6</sub> emissions due to uncertain associated gas C<sub>2</sub>H<sub>6</sub> content are also provided in Table S-16 of the Supporting Information.

Global coal industry CH<sub>4</sub> emissions (panel c) are nearly identical with EDGAR<sup>13</sup> between 1980 and 2002. Past 2002, EDGAR emissions increase at a greater rate, largely due to

higher emissions estimates in China, United States, India, and Russia. Recent global top-down studies<sup>12,22</sup> also found smaller anthropogenic CH<sub>4</sub> emissions increases than EDGAR over this period—including China<sup>22</sup>—which EDGAR largely attributes to coal mining (Figure 2c). Similar to NG and oil, differences in coal emissions for individual countries vary significantly between this work and EDGAR. In fact, emissions for 12 out of 22 countries estimated here differ by at least 25% from EDGAR (Table S-18, Supporting Information). Uncertainty estimates of coal CH<sub>4</sub> emissions are based on literature ranges of underground mining EFs. The lower and upper bounds in Figure 2 assume lower and upper bound EFs in Table 2, respectively, from all countries simultaneously. There are additional sources of uncertainty related to data quality of country-specific underground and surface mining, which are difficult to estimate. Analogous to oil, the emissions uncertainties quantified here allow a better assessment of FER uncertainties in top-down modeling. C<sub>2</sub>H<sub>6</sub> emissions and uncertainties (due to uncertain coal gas C<sub>2</sub>H<sub>6</sub> content) are shown based on our medium CH<sub>4</sub> emissions estimate. Coal C<sub>2</sub>H<sub>6</sub> emissions are minor compared to total C<sub>2</sub>H<sub>6</sub> emissions from NG and oil systems (Figure 2).

Grid maps (CH<sub>4</sub> and C<sub>2</sub>H<sub>6</sub>) that can be used for atmospheric modeling were developed for each emissions source and year based on the spatial distribution provided by EDGAR. The spatial distribution of emissions within each country were adapted from EDGAR and scaled to match the country-level emissions totals estimated above. Example grid maps are shown in Figure 3 illustrating NG CH<sub>4</sub> emissions in 2008 (last year reported in EDGAR v4.2). Note that emissions are plotted on a log scale. Panel a shows results for the medium FER scenario (3.1% global average FER; see Table S-17, Supporting Information, for details and region specific data). Panels b–d illustrate emissions differences between the low (b, 2.2% global average FER), medium (c), and high (d, 5.1% global average FER) scenarios and EDGAR v4.2. The difference maps show greater emissions compared to EDGAR v4.2 in some countries even in the low FER scenario (e.g., in the United States and Norway at 1.4% FER). The difference maps also show fewer emissions compared to EDGAR v4.2 in some countries even in the high FER scenario (e.g., in the Ukraine and Pakistan at 5.0% FER). It is difficult to explain the large differences without additional documentation in EDGAR, but use of different activity data and country reported emissions may be important factors (see details in section 7, Supporting Information). The grid maps were converted from 0.1° × 0.1° grid resolution to a lower 1° × 1° resolution, which is required for top-down modeling with NOAA's CarbonTracker-CH<sub>4</sub> assimilation system.<sup>12</sup> While EDGAR's spatial emissions distribution within each country is subject to limited data (see above), this may have only a minor influence when (i) attributing emissions sources globally<sup>10</sup> and (ii) simulating transport at 1° × 1° resolution<sup>12</sup> (e.g., approximately 110 km × 110 km in the United States).

Grid maps for oil and coal CH<sub>4</sub> emissions are shown in section 7 of the Supporting Information. Oil grid maps include emissions from tanker transport across the oceans. Coal grid maps appear incomplete due to missing information regarding the spatial emissions distribution as coal industry emissions are mainly point sources from individual mines.<sup>55</sup> These are difficult to visualize on a grid map. Grid maps for C<sub>2</sub>H<sub>6</sub> are not shown as these differ from CH<sub>4</sub> only in the legend scale.

## CONCLUSIONS

A global bottom-up FF CH<sub>4</sub> and C<sub>2</sub>H<sub>6</sub> emissions inventory was developed that can be used as *prior* estimates in top-down atmospheric modeling, for example, for reducing uncertainty in fugitive emissions from the NG industry.<sup>10</sup> Because top-down NG emissions estimates depend on *prior* bottom-up oil and coal estimates, quantifying bottom-up uncertainties is crucial. A major contribution of this work is estimating bottom-up uncertainties, which received little attention in previous work. Also, this inventory allows top-down modelers to infer FER from absolute (Tg/yr) top-down NG estimates, which is not possible using existing inventories. This inventory includes FF hydrocarbon gas composition, absolute country-specific CH<sub>4</sub> emissions from the NG, oil, and coal industries, and spatial allocation of emissions. The emphasis was on striking a balance between using detailed country-level data for the major emitting countries and allowing transparency in methods and results in order to facilitate interpretation of top-down results, particularly inferring FER from total emissions, based on assumptions underlying the emissions *priors*.

Emissions were estimated based on country-level and other EFs (oil and coal industries), hydrocarbon gas composition, and country-level FF production data from the literature. Upstream gas composition was quantified based on nearly 7000 well samples in order to estimate both CH<sub>4</sub> and C<sub>2</sub>H<sub>6</sub> emissions. Downstream gas composition was quantified through a mass balance approach using upstream NG composition as well as upstream and downstream NG and NGL production in the United States. We showed that the global average of EDGAR<sup>13</sup> *priors*—the predominantly used CH<sub>4</sub> database for top-down modeling—is equivalent to about 2.5% FER (despite significant country-level differences to this work). Furthermore, the 9% FER scenario appears unlikely high given previous top-down studies, which was investigated in more detail by Schwietzke et al.<sup>10</sup> While our global oil and coal CH<sub>4</sub> estimates coincide well with EDGAR for most years, country-level emissions vary substantially, which may influence atmospheric modeling results. Also, our global coal CH<sub>4</sub> estimates increase at a lower rate over the past decade compared to EDGAR, which is consistent with recent top-down modeling.<sup>12,22</sup> This is important because lower *prior* coal estimates increase top-down NG estimates for a given global total emissions estimate based on observational constraints.<sup>10</sup> The C<sub>2</sub>H<sub>6</sub> emissions inventory and grid maps represent a further contribution and development of the EDGAR product. This step is important because C<sub>2</sub>H<sub>6</sub> is a convenient tracer gas of FF emissions, and it is particularly useful for characterizing FER uncertainty in the NG industry. The existing global observational CH<sub>4</sub> and C<sub>2</sub>H<sub>6</sub> network is too sparse for distinguishing NG from oil and coal. As we have shown elsewhere,<sup>10</sup> the detailed *prior* emissions inventory and grid maps developed here are a useful tool in top-down modeling to make this distinction.

## ASSOCIATED CONTENT

### Supporting Information

Country-specific activity data, upstream NG composition data, literature FER review, oil and coal emissions details, grid map scaling procedure, additional model results. Total country-specific emissions and uncertainties are available in spreadsheet format under <http://cedmcenter.org/tools-for-cedm/global-fossil-fuel-fugitive-methane-and-ethane-emissions-inventory>.

This material is available free of charge via the Internet at <http://pubs.acs.org>.

## AUTHOR INFORMATION

### Corresponding Author

\*Phone: (303) 497-5073. E-mail: [stefan.schwietzke@noaa.gov](mailto:stefan.schwietzke@noaa.gov).

### Present Address

S. Schwietzke: NOAA Earth Systems Research Laboratory, 325 Broadway GMD1, Boulder, Colorado 80305, United States

### Author Contributions

S.S. was responsible for study design, model development, and manuscript preparation. W.M.G. and H.S.M. helped with study design, model analysis, and improved the manuscript. L.B. helped with model analysis and improved the manuscript. All authors have given approval to the final version of the manuscript.

### Notes

The authors declare no competing financial interest.

## ACKNOWLEDGMENTS

We thank Mitchell Small for valuable comments and discussions. This research was made possible through support from the Climate and Energy Decision Making (CEDM) Center. This Center has been created through a cooperative agreement between the National Science Foundation (SES-0949710) and Carnegie Mellon University. The ERM Foundation-North America Sustainability Fellowship has provided additional funding.

## ABBREVIATIONS

BLM, U.S. Bureau of Land Management; CH<sub>4</sub>, methane; C<sub>2</sub>H<sub>6</sub>, ethane; EF, emissions factor; FER, fugitive emissions rate (% of dry production of NG); FF, fossil fuels (natural gas, oil, coal); GWP, global warming potential; N<sub>2</sub>, nitrogen; NG, natural gas

## REFERENCES

- (1) Kirschke, S.; et al. Three decades of global methane sources and sinks. *Nat. Geosci.* **2013**, *6*, 813–823.
- (2) Myhre, G. et al. In *Climate Change 2013: The Physical Science Basis*; Working Group I of the Fifth Assessment of the Intergovernmental Panel on Climate Change; Stocker, T. F. et al.; Eds.; Cambridge University Press: Cambridge, 2014.
- (3) International Energy Statistics, 2013. U.S. Energy Information Administration. <http://www.eia.gov/cfapps/ipdbproject/iedindex3.cfm?tid=2&pid=38&aid=12&cid=regions&syid=1980&eyid=2011&unit=BKWH>.
- (4) Venkatesh, A.; Jaramillo, P.; Griffin, W. M.; Matthews, H. S. Uncertainty in life cycle greenhouse gas emissions from United States natural gas end-uses and its effects on policy. *Environ. Sci. Technol.* **2011**, *45*, 8182–8189.
- (5) Howarth, R. W.; Santoro, R.; Ingraffea, A. Methane and the greenhouse-gas footprint of natural gas from shale formations. *Clim. Change* **2011**, *106*, 679–690.
- (6) Weber, C. L.; Clavin, C. Life cycle carbon footprint of shale gas: Review of evidence and implications. *Environ. Sci. Technol. Technol.* **2012**, *46*, S688–S695.
- (7) Allen, D. T.; et al. Measurements of methane emissions at natural gas production sites in the United States. *Proc. Natl. Acad. Sci. U.S.A.* **2013**, *110*, 17768–73.
- (8) Petron, G.; et al. Hydrocarbon emissions characterization in the Colorado Front Range: A pilot study. *J. Geophys. Res.* **2012**, *117*, D04304.

- (9) Karion, A.; et al. Methane emissions estimate from airborne measurements over a western United States natural gas field. *Geophys. Res. Lett.* **2013**, *40*, 4393–4397.

- (10) Schwietzke, S.; Griffin, W. M.; Matthews, H. S.; Bruhwiler, L. M. P. Natural gas fugitive emissions rates constrained by global atmospheric methane and ethane. *Environ. Sci. Technol.* **2014**, DOI: 10.1021/es501204c.

- (11) Dlugokencky, E. J.; Nisbet, E. G.; Fisher, R.; Lowry, D. Global atmospheric methane: Budget, changes and dangers. *Philos. Trans. R. Soc., A* **2011**, *369*, 2058–2072.

- (12) Bruhwiler, L.; et al. CarbonTracker-CH<sub>4</sub>: An assimilation system for estimating emissions of atmospheric methane. *Atmos. Chem. Phys. Discuss.* **2014**, *14*, 2175–2233.

- (13) Emission Database for Global Atmospheric Research (EDGAR), release version 4.2, 2011. European Commission, Joint Research Centre (JRC)/Netherlands Environmental Assessment Agency (PBL). <http://edgar.jrc.ec.europa.eu> (accessed 2014).

- (14) Höglund-Isaksson, L. Global anthropogenic methane emissions 2005–2030: Technical mitigation potentials and costs. *Atmos. Chem. Phys. Discuss.* **2012**, *12*, 11275–11315.

- (15) Mikaloff Fletcher, S. E.; Tans, P. P.; Bruhwiler, L. M.; Miller, J. B.; Heimann, M. CH<sub>4</sub> sources estimated from atmospheric observations of CH<sub>4</sub> and its <sup>13</sup>C/<sup>12</sup>C isotopic ratios: 1. Inverse modeling of source processes. *Global Biogeochem. Cycles* **2004**, *18*, GB4004.

- (16) Wang, J. S. et al. A 3-D model analysis of the slowdown and interannual variability in the methane growth rate from 1988 to 1997. *Global Biogeochem. Cycles* **2004**, *18*, GB4004.

- (17) Nisbet, E. G.; Dlugokencky, E. J.; Bousquet, P. Methane on the rise—Again. *Science* **2014**, *343*, 493–495.

- (18) *Global Anthropogenic Non-CO<sub>2</sub> Greenhouse Gas Emissions: 1990–2030*; EPA 430-R-12-006; U.S. Environmental Protection Agency : Washington, DC, 2012.

- (19) Janssens-Maenhout, G. et al. *EDGAR-HTAP: A Harmonized Gridded Air Pollution Emission Dataset Based on National Inventories*; JRC European Commission, 2012.

- (20) Bousquet, P.; et al. Contribution of anthropogenic and natural sources to atmospheric methane variability. *Nature* **2006**, *443*, 439–43.

- (21) Chen, Y.-H.; Prinn, R. G. Estimation of atmospheric methane emissions between 1996 and 2001 using a three-dimensional global chemical transport model. *J. Geophys. Res. Atmos.* **2006**, *111*, 27.

- (22) Bergamaschi, P.; et al. Atmospheric CH<sub>4</sub> in the first decade of the 21st century: Inverse modeling analysis using SCIAMACHY satellite retrievals and NOAA surface measurements. *J. Geophys. Res. Atmos.* **2013**, *118*, 7350–7369.

- (23) Monteil, G.; et al. Interpreting methane variations in the past two decades using measurements of CH<sub>4</sub> mixing ratio and isotopic composition. *Atmos. Chem. Phys.* **2011**, *11*, 9141–9153.

- (24) Natural Gas. Definitions, Sources and Explanatory Notes. U.S. Energy Information Administration. [http://www.eia.gov/dnav/ng/TblDefs/ng\\_prod\\_sum\\_tbldef2.asp](http://www.eia.gov/dnav/ng/TblDefs/ng_prod_sum_tbldef2.asp) (accessed 2014).

- (25) Overview of Natural Gas, 2013. NaturalGas.org. <http://naturalgas.org/overview/>.

- (26) Etiope, G.; Ciccioli, P. Earth's degassing: A missing ethane and propane source. *Science* **2009**, *323*, 478.

- (27) Simpson, I. J.; et al. Long-term decline of global atmospheric ethane concentrations and implications for methane. *Nature* **2012**, *488*, 490–494.

- (28) Pilcher, R. *Personal communication*, 2012.

- (29) Aden, N. Initial Assessment of NBS Energy Data Revisions; Ernest Orlando Lawrence Berkeley National Laboratory, China Energy Group, 2010.

- (30) Guan, D.; Liu, Z.; Geng, Y.; Lindner, S.; Hubacek, K. The gigatonne gap in China's carbon dioxide inventories. *Nat. Clim. Change* **2012**, *2*, 1–4.

- (31) Dones, R.; Heck, T.; Faist Emmenegger, M.; Jungbluth, N. Life cycle inventories for the nuclear and natural gas energy systems, and

examples of uncertainty analysis. *Int. J. Life Cycle Assess.* **2005**, *10*, 10–23.

(32) Reshetnikov, A. I.; Paramonova, N. N.; Shashkov, A. A. An evaluation of historical methane emissions from the Soviet gas industry. *J. Geophys. Res.* **2000**, *105*, 3517–3529.

(33) Mitchell, C.; Sweet, J.; Jackson, T. A study of leakage from the UK natural gas distribution system. *Energy Policy* **1990**, *18*, 809–818.

(34) Segeler, G. C. *Gas Engineers Handbook*; The Industrial Press: South Norwalk, CT, 1966.

(35) Natural Gas. Natural Gas Gross Withdrawals and Production, 2013. U.S. Energy Information Administration. [http://www.eia.gov/dnav/ng/ng\\_prod\\_sum\\_dcu\\_NUS\\_m.htm](http://www.eia.gov/dnav/ng/ng_prod_sum_dcu_NUS_m.htm).

(36) Etiope, G. Personal communication, 2013.

(37) Gage, D.; Driskill, D. L. *Analyses of Natural Gases 1917–2007*; U.S. Bureau of Land Management: Washington, DC, 2008.

(38) Petroleum & Other Liquids. Natural Gas Plant Field Production, 2013. U.S. Energy Information Administration. [http://www.eia.gov/dnav/pet/PET\\_PNP\\_GP\\_DC\\_NUS\\_MBBLPD\\_A.htm](http://www.eia.gov/dnav/pet/PET_PNP_GP_DC_NUS_MBBLPD_A.htm).

(39) Aydin, M.; et al. Recent decreases in fossil-fuel emissions of ethane and methane derived from firm air. *Nature* **2011**, *476*, 198–201.

(40) National Greenhouse Gas Emissions Data, 2013. U.S. Environmental Protection Agency. <http://www.epa.gov/climatechange/ghgemissions/usinventoryreport.html>.

(41) Wilson, D.; Fanjoy, J.; Billings, R. Gulfwide Emission Inventory Study for the Regional Haze and Ozone Modeling Effort, 2004. U.S. Department of the Interior. <http://www.boem.gov/BOEM-Newsroom/Technical-Announcements/2004-072.aspx>.

(42) Wilson, D. Year 2008 Gulfwide Emission Inventory Study. U.S. Department of the Interior. [http://www.boem.gov/uploadedFiles/BOEM/BOEM\\_Newsroom/Library/Publications/2012/PowerPoint\\_Source\\_Files/3F\\_0140\\_Wilson\\_PPT.pdf](http://www.boem.gov/uploadedFiles/BOEM/BOEM_Newsroom/Library/Publications/2012/PowerPoint_Source_Files/3F_0140_Wilson_PPT.pdf).

(43) 2006 IPCC Guidelines for National Greenhouse Gas Inventories. National Greenhouse Gas Inventories Programme. <http://www.ipcc-nggip.iges.or.jp/public/2006gl/>.

(44) Petroleum & Other Liquids. This Week in Petroleum, 2013. [http://www.eia.gov/oog/info/twip/twip\\_gasoline.html#production](http://www.eia.gov/oog/info/twip/twip_gasoline.html#production).

(45) Stroscher, M. T. Characterization of emissions from diffusion flare systems. *J. Air Waste Manage. Assoc.* **2000**, *50*, 1723–1733.

(46) Gogolek, P. *Experimental Studies on Methane Emissions from Associated Gas Flares*; Natural Resources Canada, Canmet Energy: Ottawa, Canada, 2012.

(47) Parameters for Properly Designed and Operated Flares, 2012. U.S. EPA Office of Air Quality Planning and Standards. <http://www.epa.gov/ttn/atw/flare/2012flaretechreport.pdf>.

(48) Elvidge, C. D.; et al. A fifteen year record of global natural gas flaring derived from satellite data. *Energies* **2009**, *2*, 595–622.

(49) Elvidge, C. D.; Baugh, K. E.; Ziskin, D.; Anderson, S.; Ghosh, T. Estimation of Gas Flaring Volumes Using NASA MODIS Fire Detection Products, 2011. [http://ngdc.noaa.gov/eog/interest/flare\\_docs/NGDC\\_annual\\_report\\_20110209.pdf](http://ngdc.noaa.gov/eog/interest/flare_docs/NGDC_annual_report_20110209.pdf).

(50) Kotarba, M. J.; Lewan, M. D. Characterizing thermogenic coalbed gas from Polish coals of different ranks by hydrous pyrolysis. *Org. Geochem.* **2004**, *35*, 615–646.

(51) Kim, A. G. *The Composition of Coalbed Gas*; Report of Investigations 7762; U.S. Department of the Interior: Washington, DC, 1973.

(52) Reducing Methane Emissions from Coal Mines in China: The Potential for Coalbed Methane Development, 1996. U.S. Environmental Protection Agency. <http://www.epa.gov/cmop/docs/int004.pdf>.

(53) China Coal Industry Yearbook 2009. <http://www.chinabookshop.net/china-coal-industry-yearbook-2009-p-11062.html>.

(54) Claus, S.; De Hauwere, N.; Vanhoorne, B.; Hernandez, F.; Mees, J. Maritime Boundaries Geodatabase, 2012. <http://www.marineregions.org/downloads.php>.

(55) Janssens-Maenhout, G. Personal communication, 2012.